IEEE Access
Multidisciplinary ⋮ Rapid Review ⋮ Open Access Journal

Received February 16, 2020, accepted March 26, 2020, date of publication April 27, 2020, date of current version May 19, 2020.
Digital Object Identifier 10.1109/ACCESS.2020.2990759

Effect of Thickness on the Space Charge Behavior and DC Breakdown Strength of Cross-Linked Polyethylene Insulation

ZHIPENG MA, LIJUN YANG, (Member, IEEE), MUHAMMAD SHOAIB BHUTTA, HAORAN BIAN, AND MUHAMMAD ZEESHAN KHAN
State Key Laboratory of Power Transmission Equipment and System Security and New Technology, Chongqing University, Chongqing 400044, China
Corresponding author: Lijun Yang (yljcqu@cqu.edu.cn)

This work was supported by the National Key Research and Development Program of China under Grant 2016YFB0900701.

ABSTRACT In high voltage direct current (HVDC) cable systems, study of electric field distortion created by space charge accumulation is very important for examining insulation performance. Therefore, in this paper the influence of space charge on short-time breakdown characteristics of cross-linked polyethylene (XLPE) are studied. Trap energy distribution is an important factor affecting space charge behavior in dielectrics. Dielectrics with various thicknesses exhibit different space charge phenomena due to various trap distribution characteristics, which regulate the injection, migration and accumulation processes of charges. Consequently, trap characteristics can affect many parameters, such as charge accumulation depth and injection barrier. XLPE with thickness less than 100 μm show lower density of deep traps which can accumulate homogeneous bulk charges as compared to thick XLPE with thickness greater than 100 μm. This phenomenon determines the internal field strength distortion rate which is 20% larger for thin XLPE and it is much higher than that for thick XLPE. The external factor which is considered for analysis is applied field strength and it shows a linear proportional affect on the electric field distortion. A quantitative relationship model between applied field strength and distortion field strength of XLPE with different thicknesses was established. Linear extrapolation was used to obtain the trend of applied, distortion, and actual field strengths at different XLPE thicknesses when breakdown occurred. When the thickness of XLPE is less than 100 μm, distortion field strengths is higher than 50 kV/mm and increases with decreasing thickness, resulting in a significant effect on the breakdown phenomenon and breakdown strength increases with increasing thickness. And when the thickness of XLPE is greater than 100 μm, the distortion field strengths is less than 50 kV/mm which also confirms the volume effect on breakdown phenomenon and breakdown strength decreases with increasing thickness.

INDEX TERMS Breakdown, thickness, space charge accumulation, XLPE.

I. INTRODUCTION

Cross-linked polyethylene (XLPE) shows excellent insulation performance and high thermal stability. It has been widely used as an insulation material in medium, high, and ultra-high voltage DC cables[1]–[4]. Under high voltage DC electric fields, space charge accumulates inside the insulating material. This accumulation will lead to severe electric field distortion in these materials [5]–[7]. Many studies have been carried out on the phenomenon and mechanism of the electric field distortion caused by space charge accumulation. Mitsumoto *et al*. [8] showed that the strength of the distortion electric field could be larger than eight times the applied field strength. This will certainly threaten the safe operation of insulation materials. The distortion electric field needs to be considered when designing of DC cable insulation. Li and Takada [9] studied the space charge measurement of solid insulating materials. It was found that space charge accumulation depends on the material properties, temperature, electric field strength as well as mechanical stress and chemical structure. The above factors influence the aging and breakdown strength of insulating materials. Delpino *et al*. [10] pointed out that the space charge accumulation is caused by charges injected from the cathode and anode into the insulating material under an applied electric field. The accumulation of space charge around the electrodes

The associate editor coordinating the review of this manuscript and approving it for publication was Jenny Mahoney.

This work is licensed under a Creative Commons Attribution 4.0 License. For more information, see https://creativecommons.org/licenses/by/4.0/

has been widely confirmed, and related theoretical explanations and simulation studies have been reported [11]–[13]. However, the intrinsic causes of insulation failure owing to space charge accumulation have not been fully clarified.

Therefore, this paper focuses on the influence of space charge accumulation on the breakdown characteristics of XLPE with different thicknesses based on the experimental results. The main factors affecting space charge accumulation are the sample thickness and applied field strength. A quantitative relationship model between the applied field strength and distortion field strength for samples with different thicknesses is presented. Furthermore, the variations in the breakdown strength of XLPE with sample thickness under AC and DC test conditions were obtained. Finally, the regulation rule of intrinsic and external factors on the space charge behavior is analyzed. Then the influence of space charge behavior on DC breakdown characteristics is explained using the quantitative relationship model.

II. EXPERIMENTAL dETAILS

A. MATERIALS AND SAMPLE FABRICATION

The raw material of XLPE, namely, the product model LS4258DCE, used for DC cable production, was purchased from BOREALIS Co. (Austria). A plate vulcanizer was preheated at 170 °C for 10 min and XLPE was pressed at 10 MPa for 30 min on the vulcanizer. Samples with thicknesses of 50–170 μm were prepared by adjusting the module. Thicknesses of different parts of the samples were measured using a thickness gauge with accuracy up to 0.001 mm. In addition, samples with thickness differences less than 5 μm were retained to reduce the influence of sample uniformity on experimental data. Two batches of samples were prepared using the same method, labeled as group A and B. Finally, the samples were cleaned with anhydrous ethanol and dried at 60 °C for 24 h in a vacuum oven. For space charge and short-time breakdown strength measurements, the samples were divided into 13 different thicknesses at intervals of 10 μm. Each group consisted of ten samples.

B. EXPERIMENTAL TECHNIQUES

1) SHORT-TIME BREAKDOWN TEST

The short-time AC and DC breakdown experiments using *Voltage breakdown test instrument V5.5* were carried out according to the procedure given in ASTM-D149 [14]. During the experiment, the test voltage was increased uniformly at a rate of 1 kV/s until sample breakdown occurred. Most of the samples breakdown between 10 and 20 s, which meets the standard requirement of short-time breakdown experiments [15]. No less than 10 tests for samples with different thicknesses were carried out, the average breakdown strength and standard deviation of each group were calculated.

2) SPACE CHARGE MEASURMENT

The space charge characteristics of samples with different thicknesses were measured using the pulsed electro acoustic (PEA) method. The pulse module was used to generate a narrow high-voltage pulse that was applied to the sample. This high-voltage pulse created a small displacement of the space charge in the sample and a piezoelectric sensor was used to transform it into an electrical signal. Furthermore, Lab View software was used to collect the space charge distribution. The pulse module (model AVIR-1-C) used during the experiments was manufactured by AVTECH, a Canadian Company, which provided a pulse amplitude of 200 V and pulse width of 2–5 ns. The high-voltage DC module was manufactured by the Matsusada company, Japan (model AU-20R3-LC), having an output voltage range of 0-±20 kV. To improve measurement accuracy, silicone oil was used as an acoustic coupling agent. Experiments were conducted at ambient temperature (25 ± 1) °C and a relative humidity of 40 ± 2%. For comparison purposes, the shape, size, and material of the electrodes used in the PEA experiment were the same as those used in the short-time breakdown test.

3) THERMO-STIMULATED DEPOLARIZATION CURRENT MEASUREMENTS

Thermally stimulated depolarization current (TSDC) was carried out (Novocontrol technologies, Germany) to analyze the characteristics of trap distribution of XLPE. The samples with thickness of 80, 100, 120 μm were placed into the test chamber of TSDC equipment. Firstly, the temperature in the chamber was heated to 100 °C, and then the sample was started to polarize for 30 minutes under the applied voltage of 200 V. When polarization was finished, the sample was cooled down to −30 °C by liquid nitrogen and then short circuited for 30 minutes. After that, the sample was again heated to 100 °C with a heating rate of 2 °C/min, and the depolarization current was measured.

4) ISOTHERMAL SURFACE POTENTIAL DECAY MEASURMENT

The characteristics of carrier mobility were calculated using the isothermal surface potential decay (ISPD) method. The corona generated by the needle electrode (connected to the high voltage DC source) passed through the grid electrode to charge the sample. After charging, the samples were put under the Kelvin type probe and its surface potential was measured. The data of surface potential decay process were recorded in a computer. Experiments were conducted at ambient temperature (25 ± 1) °C and a relative humidity of 40 ± 2%.

III. EFFECT OF THICKNESS ON SPACE CHARGE AND TRAP CHARACTERISTICS OF XLPE

A. TRAP DISTRIBUTION CHARACTERISTICS OF SAMPLES WITH DIFFERENT THICKNESSES

The TSDC measurement results of samples with thickness of 80, 100, 120 μm shows in Fig. 1. It can be seen from this figure that the relaxation peak of the TSDC current occurs in the test result of samples with different thicknesses in interval of −30–100 °C. In order to extract the trap parameters

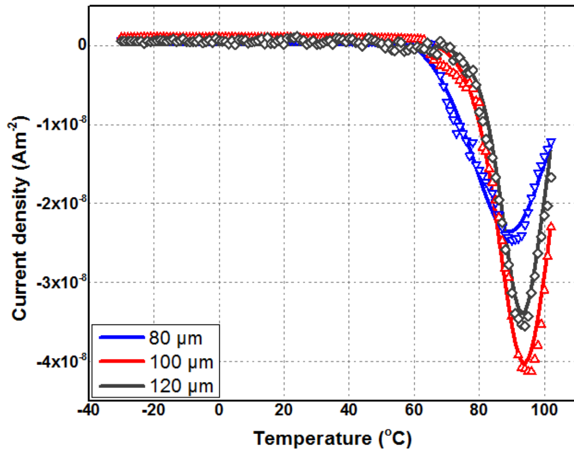

FIGURE 1. Thermally stimulated depolarization current fitting and measurement results of samples with different thicknesses.

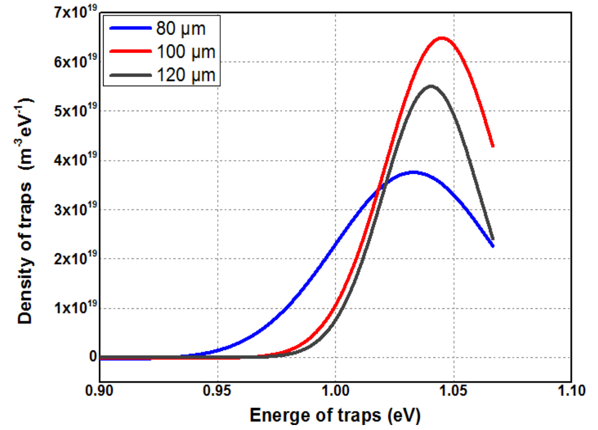

FIGURE 2. Trap depth distribution of samples with different thicknesses.

of samples, experimental results were analyzed by TSDC equation [16].

$$j_{tsc}(T) = A\exp[-\frac{E_0}{k_B T} - \frac{1}{\beta\tau_0}\int_{T_0}^{T_1}\exp\left(-\frac{E_t}{k_B T}\right)dT] \quad (1)$$

where $j_{tsc}(T)$ is the TSDC current density in Am^{-2}, A is an undermined constant in Am^{-2}, E_0 is the activation energy of relaxation process in eV, τ_0 is the relaxation time constant in s, β is heating rate in $°Cs^{-1}$, k_B is the Boltzmann constant, T_0 is the initial temperature of sample at the beginning of heating process in °C, and T_1 is the temperature of sample after heating in °C. In order to obtain the parameters of (1), the TSDC test results are fitted, and the fitting curve is in good agreement with the test results, as shown in Fig. 1.

According to TSDC theory, the distribution of trap depth and density can be calculated from the experimental results. Tian *et al.* [17] used (2) and (3) to obtain trap depth distributions form the TSDC measurement results directly. This paper calculated the trap parameters with this method.

$$E_t = k_B T\ln[v(T-T_0)/\beta] \quad (2)$$

$$f_0 N_t = \frac{2dv(T-T_0)}{k_B Tel^2\beta}J(T) \quad (3)$$

where E_t is the trap depth in eV, N_t is the trap density in $m^{-3}eV^{-1}$, ν is the escape frequency of trapped electrons, f_0 is the initial occupancy of a trap level and is a constant, e is the electronic charge quantity, d is the thickness of sample in m, l is the penetration depth of the injected electrons. Fig. 2 shows the trap depth distribution curves of samples with different thicknesses.

The peak of these curves in Fig. 2 can be compared to analyze the trap parameters of samples with different thicknesses. Trap depth of three peaks of 80, 100, and 120 μm are 1.033 eV, 1.045 eV and 1.040 eV, respectively. The trap density corresponding to each peak also has a similar relationship. As shown in Fig. 2, the order of trap density is 100 μm sample> 120 μm sample> 80 μm sample.

TABLE 1. Settings for ISPD tests.

d	Positive corona charging		Negative corona charging	
	Needle electrode	Grid electrode	Needle electrode	Grid electrode
80 μm	7.6 kV	3 kV	-7.6 kV	-3 kV
100 μm	8.8 kV	3 kV	-8.8 kV	-3 kV
120 μm	10 kV	3 kV	-10 kV	-3 kV

Carrier traps in polymers can be divided into physical and chemical traps. A physical trap is caused by the bending, folding or local arrangement of the molecular chain in the polymer, which shows a low trap depth (0.15 eV–0.3 eV). A chemical trap is caused by impurities, cross-linking byproducts and defects of the polymer molecular chain, such as in-chain or in-branch nonconjugated carbon double bonds, the side-chain carbonyl group, and end groups. Chemical trap shows a high trap depth (approximately 1 eV) [18]. Therefore, in Fig. 2, the trap depth is in the interval of 0.95 eV–1.10 eV, which belongs to the deep trap.

Fig. 2 also shows that both 100 μm and 120 μm samples have high trap density or deeper trap depth than 80 μm sample. This may be because the formation of chemical defects is affected to some extent by the size of materials. XLPE with a large thickness or size contains many impurities, cross-linking byproducts and other chemical defects. These conditions result in high trap density or deep trap depth for samples with large thickness.

B. ESTIMATION OF CARRIER MOBILITY FROM ISPD RESULTS

ISPD test method was used to measure the decay behavior of the deposited charge on the surface of the material under isothermal condition to obtain carrier mobility of the material. In the experiment, the corona produced by the needle electrode was used to charge the sample for 10 min. The test time of surface potential is more than 5000 s and the sampling frequency is 1 Hz. The voltage settings of needle electrode and grid electrode under positive and negative corona conditions are shown in Table 1.

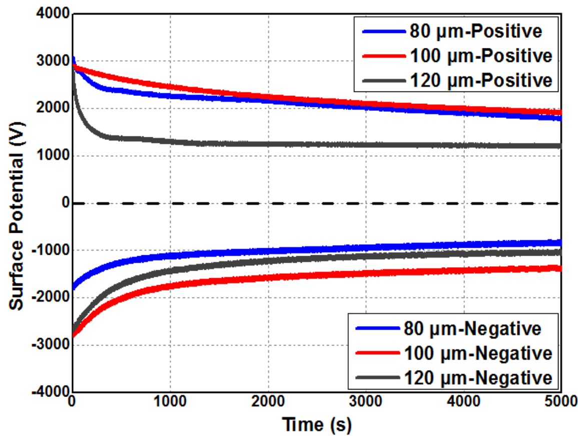

FIGURE 3. ISPD test results of samples with different thicknesses.

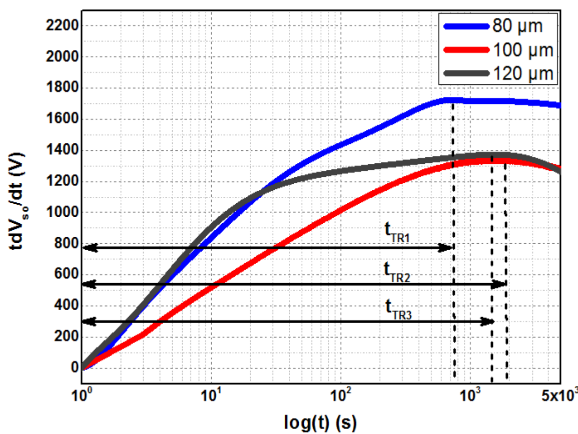

FIGURE 4. Relationship between tdV_{S0}/dt and log(t) for positive surface potential.

Fig. 3 shows the ISPD test results of XLPE samples with different thicknesses. It shows the surface potential decays over time. In the process of applied positive and negative charging voltage, charges are accumulated on the surface of the sample. Potential are formed on the surface and electric field are formed in the bulk of the material. The surface potential decay occurs because of carrier migration. The charge accumulated on the surface migrates to the ground electrode through the bulk of dielectric. The change of carrier mobility during charging process leads to the variety of surface potential decay rate [19]. In Fig. 3, different surface potential decay trends indicate that the carrier mobility of samples with various thicknesses is different.

The transit time t_{TR} is defined as the time taken for the leading charge carriers to arrive at the ground electrode. t_{TR} is estimated by fitting the results of potential decay curves with exponential function, and then the relationship between tdV_{S0}/dt and log(t) was obtained, as shown in Fig. 4 and Fig. 5. The time corresponding to the peak can be regarded as the transit time t_{TR}, and the carrier mobility determined by shallow traps can be calculated using the following equation [19].

$$\mu_{0(e,h)} = d^2 \Big/ V_{S0} \times t_{TR} \tag{4}$$

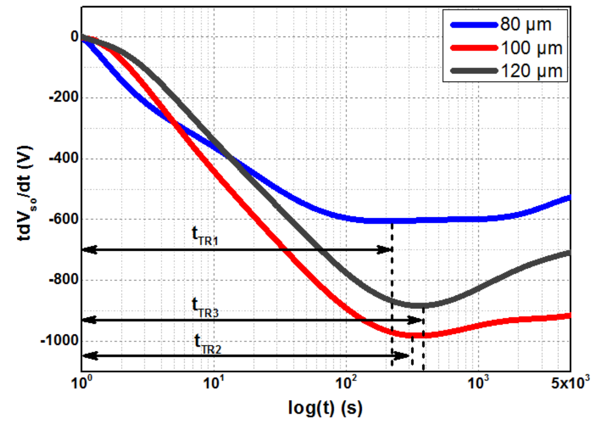

FIGURE 5. Relationship between tdV_{S0}/dt and log(t) for negative surface potential.

TABLE 2. Hole and electron carriers mobility.

	d	V_{S0}	t_{TR}	$\mu_{0(e,h)}$
Hole carrier	80 μm	7.6 kV	704 s	1.20×10^{-15} m^{2}V^{-1}s^{-1}
	100 μm	8.8 kV	1763 s	6.45×10^{-16} m^{2}V^{-1}s^{-1}
	120 μm	10 kV	1533 s	9.39×10^{-16} m^{2}V^{-1}s^{-1}
Electron carrier	80 μm	7.6 kV	196 s	4.30×10^{-15} m^{2}V^{-1}s^{-1}
	100 μm	8.8 kV	295 s	3.85×10^{-15} m^{2}V^{-1}s^{-1}
	120 μm	10 kV	358 s	4.02×10^{-15} m^{2}V^{-1}s^{-1}

where $\mu_{0(e,h)}$ is the carrier mobility determined by shallow traps in $m^2V^{-1}s^{-1}$, V_{S0} is the absolute of initial surface potential in V.

Table 2 shows the calculation results of hole and electron carriers mobility of samples with different thicknesses, respectively. The results in Table 2 shows that among the three kinds of thickness samples, the carrier mobility of 80 μm sample is the maximum, while that of 100 μm sample is the minimum.

The migration of carriers into the bulk of dielectric is related to the trap distribution characteristics. The probability of carriers bound by traps in dielectrics with high trap density or depth increases, hence these dielectrics have low carrier mobility. It can be seen from Table 2 that the mobility of carriers in the 100 μm sample is the minimum because the deep traps of this sample have high trap density and deep trap depth as shown in Fig. 2. Similar analysis can be carried out to explain the result that the carrier mobility of 80 μm sample is the maximum.

C. SPACE CHARGE ACCUMULATION CHARACTERISTICS OF SAMPLES WITH DIFFERENT THICKNESSES

The trap distribution characteristics of XLPE not only affects the carrier migration process, but also determines the space charge accumulation characteristics. Moreover, the influence of the space charge accumulation behavior, especially the transient accumulation characteristics, on the DC breakdown characteristics of XLPE samples with different thicknesses deserves further study.

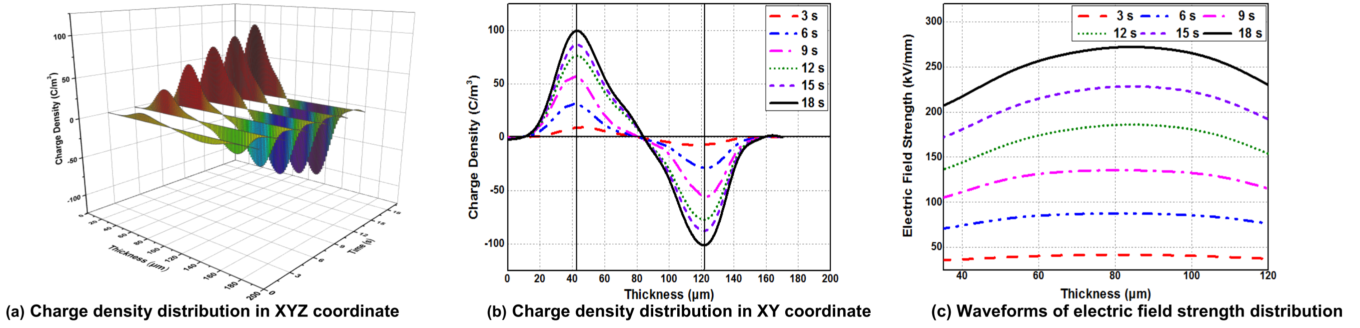

(a) Charge density distribution in XYZ coordinate (b) Charge density distribution in XY coordinate (c) Waveforms of electric field strength distribution

FIGURE 6. PEA test results of 80 μm sample.

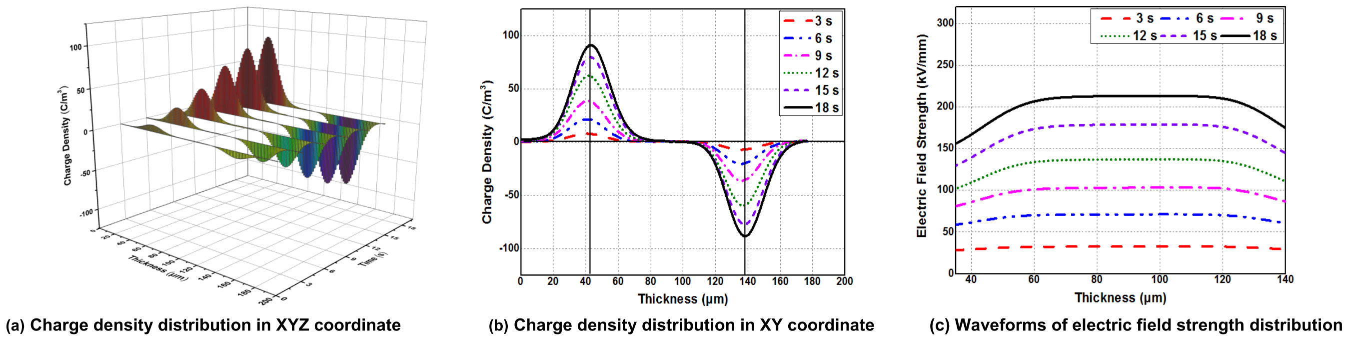

(a) Charge density distribution in XYZ coordinate (b) Charge density distribution in XY coordinate (c) Waveforms of electric field strength distribution

FIGURE 7. PEA test results of 100 μm sample.

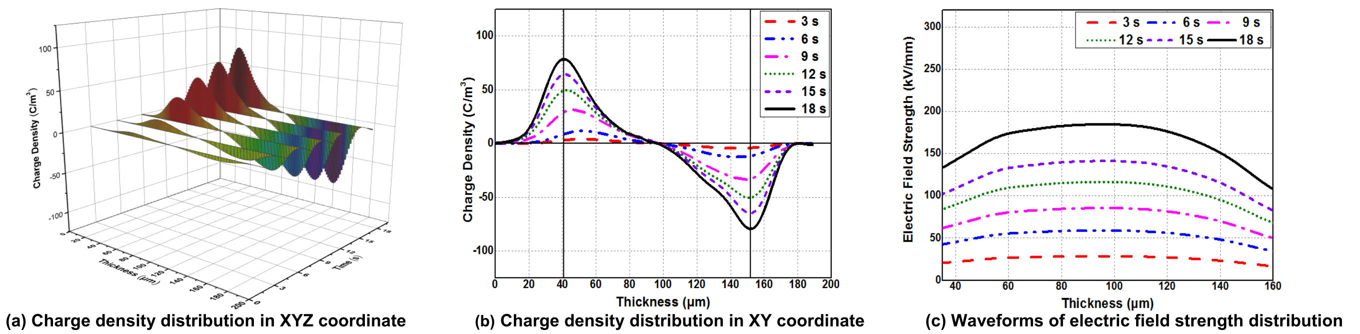

(a) Charge density distribution in XYZ coordinate (b) Charge density distribution in XY coordinate (c) Waveforms of electric field strength distribution

FIGURE 8. PEA test results of 120 μm sample.

The DC breakdown process of XLPE is transient, during which there is a rapid change of space charge accumulation behavior. This behavior is of great significance to the study of breakdown characteristics, hence some researches working on the transient accumulation behavior of space charge have been carried out. Some research methods are as follows: carry out the PEA test in the process of increasing voltage at a constant speed, and analyze the space charge density distribution curve from the beginning of increasing voltage to the near breakdown time. If the resolution of the detection device meets the test requirements, the influence of the transient accumulation characteristics of space charge on the breakdown is obtained by analyzing as many curves of charge density as possible. In [20] the space charge fast dynamic measurement with an interval of 10 μs was carried out, and the measurement duration of the test system was 1 ms. In [21] the sampling interval of PEA test equipment was 0.1 s, and the test time was 120 s.

In order to study the space charge transient accumulation characteristics of XLPE in the process near to breakdown, the XLPE samples with different thicknesses of 80, 100, 120 μm were selected for PEA test under the linearly increasing applied voltage. The minimum resolution of the PEA device used in this paper is 10 μm, and the typical thickness of the tested samples is 50 μm to 20 mm [22], [23]. This means that the detection equipment can clearly distinguish the charge density curve of the sample with the minimum thickness of 50 μm. The test voltage is increased uniformly at a rate of 1 kV/s, the same as short-time breakdown test. Since the upper limit of test voltage is 20 kV, the measurement was carried out for 20 s, and test data were obtained at sampling interval 3 s. The PEA test results are shown in Fig. 6 to Fig. 8.

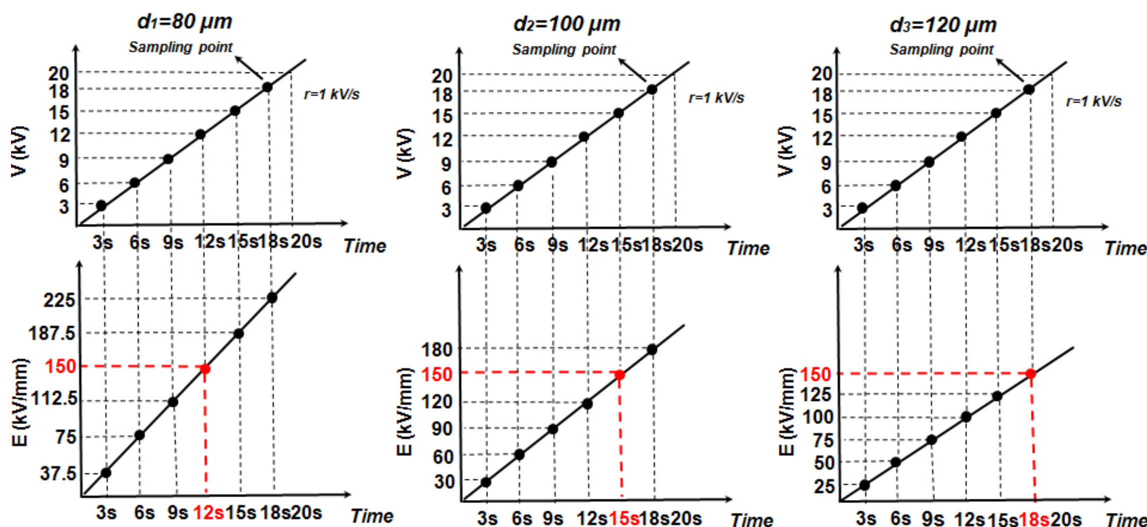

FIGURE 9. Sampling method in the PEA test.

In the part (a) of Fig. 6 to Fig. 8, the charge density are described using color scale at different sampling times. Blue and red colors indicate the negative and the positive charge densities, respectively. The charge density shows an obvious trend of increasing with the test voltage increased form 0 kV to 20 kV. Although the charge density of three kinds of thickness samples has similar increasing trends, however, for some parts of the charge density curve, especially the bulk space charge accumulation behavior of samples, there are differences which can be clearly reflected in part (b) of Fig. 6 to Fig. 8.

The charge density curves of XLPE samples with thickness of 80, 100 and 120 μm are shown in Fig. 6(b), Fig. 7(b), and Fig. 8(b), respectively. The results show that the applied voltage has a positive correlation with the accumulated space charge density. Therefore, the charge density curves has an obvious upward trend. In addition, the charge density curve shows the law of space charge accumulation in the process of increasing voltage, which has more meaningful information. During the test voltage linearly increased, the homogeneous charges accumulate on the electrode surface for a short time and migrate quickly into the bulk of sample. In fact, the thickness of the interface charge layer between electrode and dielectric is very small and there is no definite conclusion. In an ideal situation, more attention can be paid to the bulk of material, especially tow parts: the part near the electrode and the middle part of the bulk.

Fig. 6(b), Fig. 7(b), and Fig. 8(b) show some obvious differences in the middle part of the charge density distribution curves of the samples with three kinds of thicknesses. The middle part of charge density curve of 100 μm sample is flatter than that of 80 μm and 120 μm samples, which indicates that less amount of space charge accumulated in the bulk of 100 μm sample during the test voltage linearly increased. In this paper, the charge density curves of samples

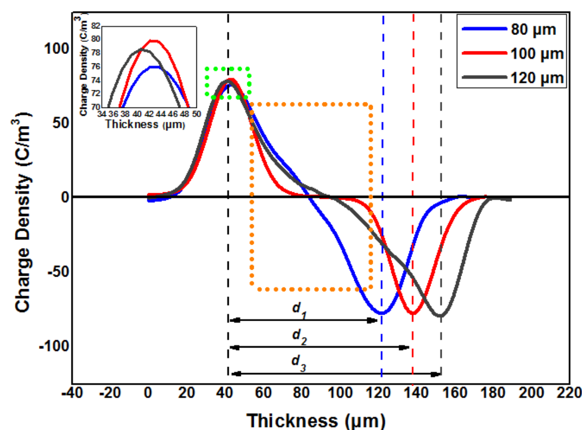

FIGURE 10. Space charge density distribution curves of samples under 150 kV/mm.

with three kinds of thickness are compared under the same field strength for further analysis. As shown in Fig. 9, the test voltage was increased at the rate of 1 kV/s, and the space charge was measured every 3 second. The voltage at each sampling point is obtained in 0–20s as follows: 3 kV, 6 kV, 9 kV, 12 kV, 15 kV and 18 kV respectively.

At each sampling point, the applied field strength for the samples with various thicknesses is different when the voltage is applied to the samples. This is because when the increasing voltage applied on 80, 100 and 120 μm samples at rate of 1 kV/s, the rate of increasing field strength of each sample is different. After sampling, the field strength of each sampling point for different thicknesses samples is various, as shown in Fig. 9. However, we can find the same field strength that can be sampled in all three kinds of thickness samples, that is 150 kV/mm. Therefore, the space charge density curves of three kinds of thickness samples under 150 kV/mm was chosen for further analysis, as shown in Fig. 10.

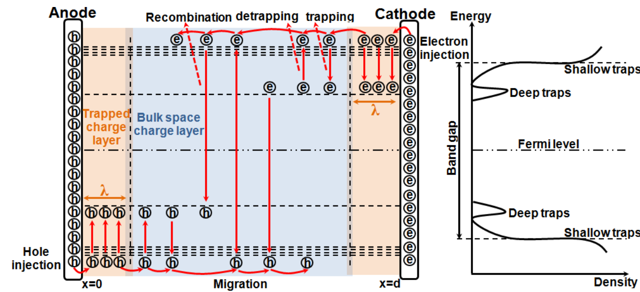

FIGURE 11. Schematic of charge transport model.

Fig. 10 shows that the charge density at the peak of the three curves, can be obtained: 76.03 C/m^3 (80 μm sample), 79.83 C/m^3 (100 μm sample) and 78.82 C/m^3 (120 μm sample), which are similar. It can be inferred that the amount of charge accumulated around the interface have no obvious difference for the three kinds of thickness samples under the same field strength of 150 kV/mm. However, the order of the peak values of the three charge density curves can not be ignored. The curves in the green rectangle of Fig. 10 show that the order of charge density value at peaks is 100 μm sample> 120 μm sample> 80 μm sample.

We focus on the middle part of the charge density distribution curves of the samples in Fig. 10. In most of this region, the charge density curve of 100 μm sample is flat and that of 80 μm sample and 120 μm sample are uneven. Moreover, it can be seen clearly that in the orange rectangle of Fig. 10, the order of charge density value is 80 μm sample > 120 μm sample > 100 μm sample. This means that, in this region of sample, the homogeneous bulk charge accumulated in 80 μm sample is more than that in 100 μm and 120 μm samples. The homogeneous bulk charge accumulated in 100 μm sample is the least among the three kind of thickness samples.

It can be concluded that the space charge accumulated in the middle bulk of samples decrease obviously with an increase in the density of deep trap, while the space charge accumulated around the interface between sample and electrode increase slightly, by comparing the order of charge density and trap density of three kinds of thickness samples. This phenomenon can be attributed that the accumulation behaviors of space charge in bulk of dielectric is regulated by trap characteristics and carrier migration behaviors. Specifically, the space charge behavior depends on the balance between the charge injection process and the bulk conduction process, both of which are affected by the material trap characteristics [24], [25]. Charge transport model, such as bipolar space charge controlled electrical breakdown model, is usually been used to analyze this phenomenon. The schematic for charge transport model for the dielectric under applied DC field is presented in Fig. 11 [24].

The charge transport model consists of injection, migration, trapping/detrapping of electrons and holes, and recombination between electrons and holes [25]. Some parameters of the material can affect the above processes, such as: the injection of charge is determined by the injection barrier and interface electric field; the migration of charge is determined by the charge carrier mobility and electric field; the trapping of charge is determined by the trap density and depth; the detrapping of charge is determined by the trap depth and electric field.

It is an important condition for accumulation space charge in the bulk that the charge is injected from the electrode faster than it is conducted across the bulk. Under this condition, the charge trapping process is stronger than the detrapping process. Most of the charges injected from the electrode can be trapped and then forms trapped charge layer around the interface, as shown in Fig. 11. The trapped charge layer forms a opposite electric field, which weakens the field strength around the interface. Hence, higher field strength is needed to overcome this weakening effect to exceed the charge injection potential barrier φ. It is equivalent to raises the value of φ, resulting in the weakening of the charge injection process. The weakening effect will affect charge migration and accumulation processes. The injection current decreases (the charge injection rate decreases) gradually, which leads to the decrease of the difference between the injection current and the conduction current. When the rate of charge injection into the bulk of dielectric is less than the rate of charge migrated through the bulk, few charges can accumulate in the bulk. Moreover, the field strength in the bulk of dielectric enhanced by the homogeneous charge accumulated in the trapped charge layer.

It is clear that the trapped charge layer can regulate the charge injection, migration and accumulation processes analyzed above. In fact, one of the important determinants of the trapped charge layer is the trap characteristics of materials. The trap density and trap depth affect the trapped charge layer by regulating the charge accumulation depth λ, as shown in Fig. 11.

Fig. 12 shows the energy level diagram of the interface when the ohmic contact occurred between electrode and dielectric, where E_{vac} is the vacuum level, E_c is the conduction band level, E_F is the Fermi level, φ is the charge injection potential barrier, λ is the charge accumulation depth.

The electric field with the strength of E works on the injection charge. At the distance of x from the interface, the charge over crosses the injection barrier φ, then the injection process is completed. The injection barrier φ can be considered as energy of the bottom of the conduction band E_c respect to the electrode Fermi level E_F. The distance x is regulated by trap density N_t and trap depth E_t and has the following relationship with φ as shown by (5) [26].

$$x = \left(\frac{2k_B T \varepsilon_r \varepsilon_0}{e^2 N_t}\right)^{1/2} \sin^{-1}\left\{\exp\left[\frac{\varphi - (\varphi_i - \chi)}{2k_B T}\right]\right\} \times \exp\left(\frac{\varphi_i - \chi - E_t}{2k_B T}\right) \quad (5)$$

where ε_0 is the vacuum dielectric constant, ε_r is the relative dielectric constant of the insulating material, φ_i is work function of dielectric, χ is electron affinity of dielectric. When the

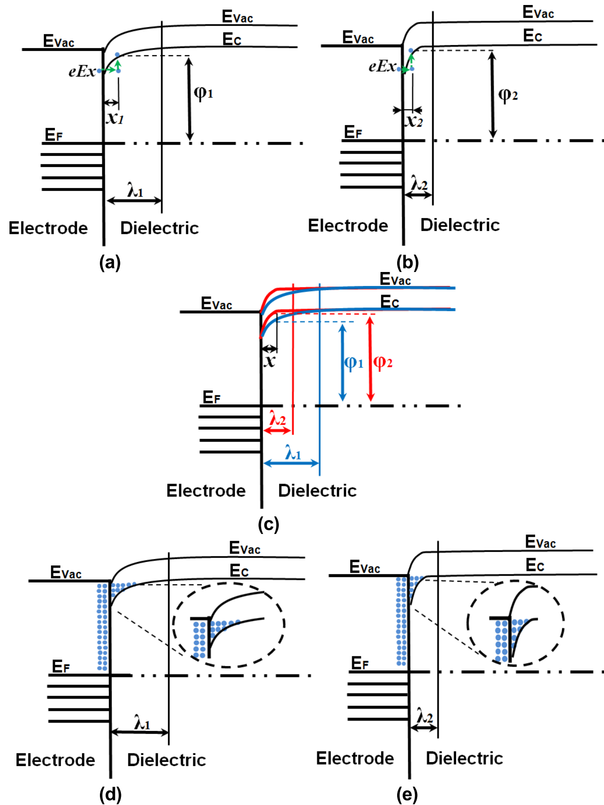

FIGURE 12. Energy level diagram of the interface when ohmic contact occurred.

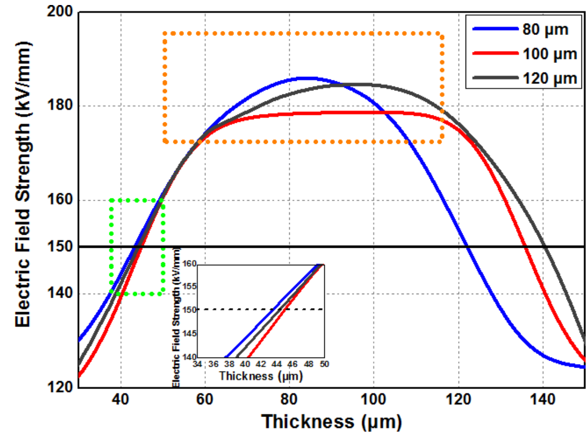

FIGURE 13. Electric field strength distribution curves of samples under 150 kV/mm.

distance x equals charge accumulation depth λ, then $\varphi = \varphi_i - \chi$, λ can be expressed as (6).

$$\lambda = \frac{\pi}{2}\left(\frac{2k_B T \varepsilon_r \varepsilon_0}{e^2 N_t}\right)^{1/2} \exp\left(\frac{\varphi_i - \chi - E_t}{2k_B T}\right) \quad (6)$$

This formula reflects the law of the trap characteristics regulate the accumulation depth of injection charge, that is, λ decreases with an increase in trap density N_t and trap depth E_t. As shown in Fig. 12(a) and Fig. 12(b), the dielectric with low trap density or shallow trap depth, named Dielectric I, has accumulation depth λ_1, and the dielectric with high trap density or deep trap depth, named Dielectric II, has accumulation depth λ_2, where $\lambda_2 < \lambda_1$. The energy level diagrams of Dielectric I and Dielectric II are compared in Fig. 12(c). As shown in Fig. 12(c), in the trapped charge layer, the charge injection barrier of Dielectric I is lower than that of Dielectric II, that is, $\varphi_1 < \varphi_2$. The charge injection barrier increases with an increase in trap density and trap depth as analyzed above. It can be inferred that the charge injection rate in Dielectric II are less than that in Dielectric I because the barrier of Dielectric II is higher than that in Dielectric I ($\varphi_1 < \varphi_2$). Hence the charge accumulation depth of Dielectric II is less than that of Dielectric I, which conforms to the assumption in Fig. 12 that $\lambda_2 < \lambda_1$. Obviously, the regulation rule of the trapped charge layer width by the trap characteristics is the same as that of the charge accumulation depth. As shown in Fig. 12(d) and Fig. 12(e), the trapped charge layer width decreases with an increase in trap density and trap depth. This means that the dielectric with high trap density and deep trap depth accumulates less bulk space charge.

The regulation rule between the test results for 80, 100 and 120 μm samples, such as trap characteristics (Fig. 2) and charge density distribution curves (Fig. 10), is consistent with the above theoretical analysis. Compared with 80 and 120 μm samples, 100 μm sample has highest trap density and deepest trap depth. This means that it has the least charge accumulation depth and the highest injection barrier, which results in the fewest space charge injected and accumulated in the bulk. Conversely, compared with 100 and 120 μm samples, it can be explained that the 80 μm sample has the strongest bulk space charge accumulation.

The process of charge injection from the electrode and accumulation in the bulk of dielectric can also be explained from the perspective of space charge effects on the electric field strength where around the interface and inside the bulk. According to the JB/T 12927-2016 standard for measuring space charge distribution in solid insulating materials [27], the electric field distribution $E(x, t)$ can be obtained using (7). If the x-axis represents the thickness direction of the sheet sample and the charge density in the sample is $\rho(x, t)$ at time t, then, at time t, the relationship between the charge density $\rho(x, t)$ and electric field distribution $E(x, t)$ can be determined using the Poisson's equation as follows:

$$E(x, t) = \frac{1}{\varepsilon_0 \varepsilon_r} \int \rho(x, t) dx \quad (7)$$

Therefore, through the PEA test, the waveform of the electric field distribution can be obtained integrally based on the waveform for charge density. Fig. 13 shows the electric field distribution waveforms of samples with thickness of 80, 100, 120 μm under the applied field strength of 150 kV/mm.

Fig. 13 can be combined with the charge density curves in Fig. 10 for analysis. In Fig. 10, the thickness interval corresponding to the green rectangle represents the region around the interface, and the thickness interval corresponding to the orange rectangle represents the region inside the

sample bulk. The rectangles with the same definition are also drawn in Fig. 13, and the field strength waveform is divided into this two regions.

Fig. 13 shows part of the electric field waveform curves in the green rectangle are less than the applied field strength (150 kV/mm). This result confirms the previous inference that the opposite electric fielded formed by the trapped charge layer weakens the field strength around the interface. The weakening degree of samples with different thicknesses is various, the field strength reduction of 100 μm sample is the largest and that of 80 μm sample is the least. The injection current density j_{in} is positively related to the electric field strength around the interface according to Schottky emission law. The injection current density of carrier can be expressed by (8).

$$j_{in}(t) = AT^2 \exp\left(-\frac{e\varphi}{k_B T}\right) \exp\left(\frac{e}{k_B T}\sqrt{\frac{eE(0,t)}{4\pi\varepsilon_r\varepsilon_0}}\right) \quad (8)$$

where $j_{in}(t)$ is the injection current density, A is the Richardson constant, $E(0,t)$ is the interface electric field.

It can be seen from (8) that the weakened interface electric field will cause the decrease of the injection current density. Therefore, the 100 μm sample with the least interface field strength should have the least injection current density. The 100 μm sample will take the lead in changing the conditions for accumulation space charge in the bulk that the charge is injected from the electrode faster than it is conducted across the bulk. The charge injection process is suppressed. Gradually, the least space charge accumulated inside the bulk of 100 μm sample as shown in Fig. 13. This causes the electric field distortion inside of the 100 μm samples bulk to be less than that of 80 and 120 μm samples as shown in orange rectangle of Fig. 13. Comparing the internal maximum field strength and applied field strength, the maximum field strength distortion rate of 80, 100, 120 μm sample is 23.3%, 18.7% and 22.7%, respectively. The low space charge injection and bulk field strength result in low carrier migration of the 100μm sample, as shown in Table 2.

Obviously, the two analysis perspective, the regulation of trap characteristics on charge behavior and influence of space charge on field strength, can be unified. Take 100 μm sample as an example, it has the highest trap density and depth and the least field strength around the interface compared with 80 and 120 μm samples. The high trap density and depth result in the small accumulation depth and trapped charge layer width. This results in the high injection barrier, and more charges only accumulate around the electrode. Then opposite electric field has strong weakening effect on the applied field strength which suppress charge injection process, resulting in the low injection current density. Hence the least space charge accumulation and electric field distortion can be found inside the bulk of 100 μm sample. On the other hand, the results of 80 μm sample can be explained by similar analysis.

As analyzed above, the XLPE samples with various thicknesses have various trap characteristics, which leads to different space charge accumulation characteristics under the same applied field strength. The electric field distortion inside of the dielectric bulk shown in Fig. 13 is an intuitive representation of space charge behavior, and also an important factor affecting the DC breakdown characteristics of XLPE. Therefore, it is necessary to further investigate the influence of space charge accumulation characteristics of XLPE with different thicknesses on DC breakdown characteristics.

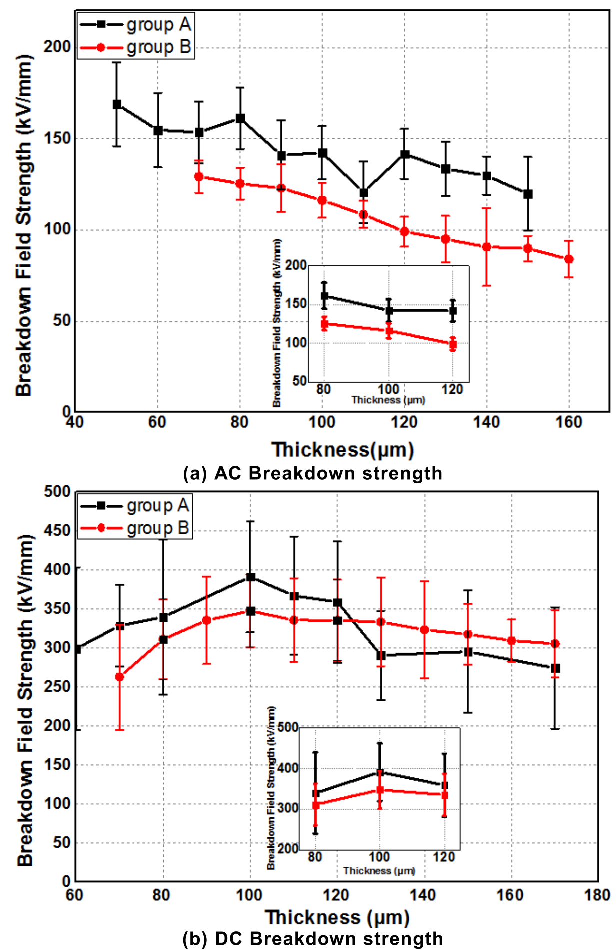

FIGURE 14. Variation of breakdown strength with thickness under (a) AC and (b) DC electric fields.

IV. EFFECT OF SPACE CHARGE ACCUMULATION ON BREAKDOWN STRENGTH

A. EFFECT OF THICKNESS ON SHORT-TIME AC AND DC BREAKDOWN CHARACTERISTICS OF XLPE

Fig. 14 shows the variations in the AC and DC breakdown strengths with different sample thicknesses from 50–170 μm. The test results of 80, 100 and 120 μm samples were drawn separately and shown in the second layer of each figure.

It can be clearly seen that the breakdown strength (E_b) varies with thickness, which is obviously different under the action of applied electric fields. Under an AC electric field, the breakdown strength E_{b-ac} decreases continuously with an increase in the thickness, whereas under a DC electric field, the breakdown strength E_{b-dc} increases first and then

decreases, showing the maximum breakdown strength at a sample thickness of 100 μm. The variation rule of breakdown strength with thickness is consistent in the results of group A and B, although there are some differences in their values due to the sample preparation of different operators.

Breakdown of solid dielectrics always occurs at their weak points that are caused by local defects [28], [29]. Based on the volume effect principle of solid dielectrics, increasing the thickness or area of the sample will lead to an increase in its volume and increase probability of local defects reduce the breakdown filed strength. Therefore, the non-uniform electric field generated at the defect site is more vulnerable to the occurrence of insulation breakdown. Thus, the breakdown strength is strongly dependent to thickness and normally decreases with the increasing thickness [30]–[32].

It can also be explained by using the volume effect principle which shows the variation in the breakdown strength with sample thickness under AC electric field. However, some of the results under DC electric field do not match this principle well. The E_{b-dc} increases with the increasing thickness in the interval of $d < 100$ μm but decreases in the interval of $d > 100$ μm.

Similar phenomena also appear in other research results. In [31], the DC breakdown characteristics of XLPE was researched. The results proved that the E_{b-dc} initially increased and subsequently decreased. The 160 μm sample approached the maximum value of E_{b-dc}, which was 5% larger than that of 100 μm sample. In [33], the thickness dependence of the breakdown characteristics of polyester film under AC and DC was investigated. The results indicated that E_{b-dc} increased from 402.5 kV/mm at $d = 40$ μm to 417.5 kV/mm at $d = 50$ μm and then decreased to 318.2 kV/mm at $d = 110$ μm.

Some studies analyzed the reason of similar phenomena.

In [34], the increase of E_{b-dc} was ascribed to the increase of crystallinity and the absence of spherulites of material. In [35], it was ascribed to the low free volume or electron mean free path in the thin film. These investigations were based on hypothesis and conjectures, and lack of more adequate tests. However, it's clear from these results that except volume effect, other factors may play a dominant role in DC breakdown, especially for thin samples and with high electric fields.

According to the analysis in the previous section, the electric field distortion inside the bulk of dielectric caused by space charge behavior is also one of the factors affecting the breakdown characteristics of insulation under DC. For example, 100 μm sample has the highest trap density and trap depth compared with 80 and 120 μm samples. That causes the least charge accumulation depth and bulk space charge accumulation. Therefore, the distortion field strength of 80 and 120 μm samples are larger than that of 100 μm sample under the same applied field strength (150 kV/mm), according to the Poisson's equation. The electric field inside the bulk of 80 and 120 μm samples are faster to reach the intrinsic breakdown field strength of XLPE than that of 100 μm sample. It can be inferred this will lead to the DC breakdown field strength of 80 and 120 μm samples are less than that of 100 μm samples, which agrees the result in Fig.14 (b).

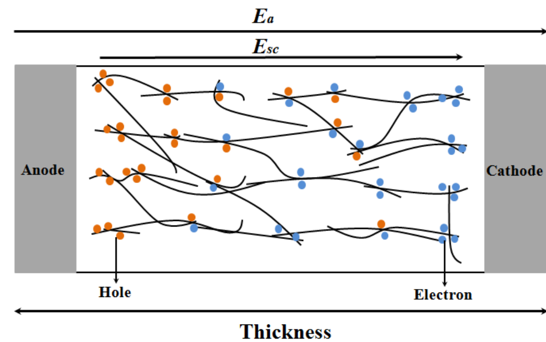

FIGURE 15. Schematic of the internal electric field formed by the accumulation of space charge.

For the test samples with more thickness kinds, the results that E_{b-dc} decreases with increasing thickness in the interval of $d > 100$ μm is in accordance with the volume effect. Meanwhile, the test results that E_{b-dc} increases with increasing thickness in the interval of $d < 100$ μm implies that the high distortion field strength caused by space charge accumulation inside thin samples at high applied field strength is the cause of this phenomenon, as reflected preliminarily by the results of the 80, 100 and 120 μm samples. This finding is confirmed further by the test results in the next section.

B. ANALYSIS OF THE RELATIONSHIP BETWEEN APPLIED AND INTERNAL ELECTRIC FIELD STRENGTHS AND SAMPLE THICKNESS

Fig. 15 shows that the applied electric field on the XLPE sample is E_a, and the maximum electric field strength due to bulk space charge accumulation is E_{sc}. Under the action of a DC electric field, the distortion field strength which is in the same direction as the applied field strength, is produced by the accumulation of space charge. Therefore, in the process of breakdown, the actual field strength of sample E_{real}, is not the applied field strength. When E_{real} is used to indicate the actual field strength of the sample, E_{real} should be considered as the parameter to analyze the effect of space charge accumulation on insulation breakdown strength.

Because of space charge accumulation, the actual electric field (E_{real}) of the sample should be the superposition of the applied electric field (E_a) and distortion electric field (E_{sc}) satisfy the relationship shown in (9).

$$E_{real} = E_a + E_{sc} \tag{9}$$

It can be inferred from (9) that the effect of E_a on E_{real} is reflected by the distortion electric field formed by space charge accumulation, but the thickness is also one of the factors regulating E_{sc}. To clarify the influence of the sample thickness and E_a on E_{real}, samples with different thicknesses under different applied electric field strengths were tested in this section. For comparing the results of the space charge

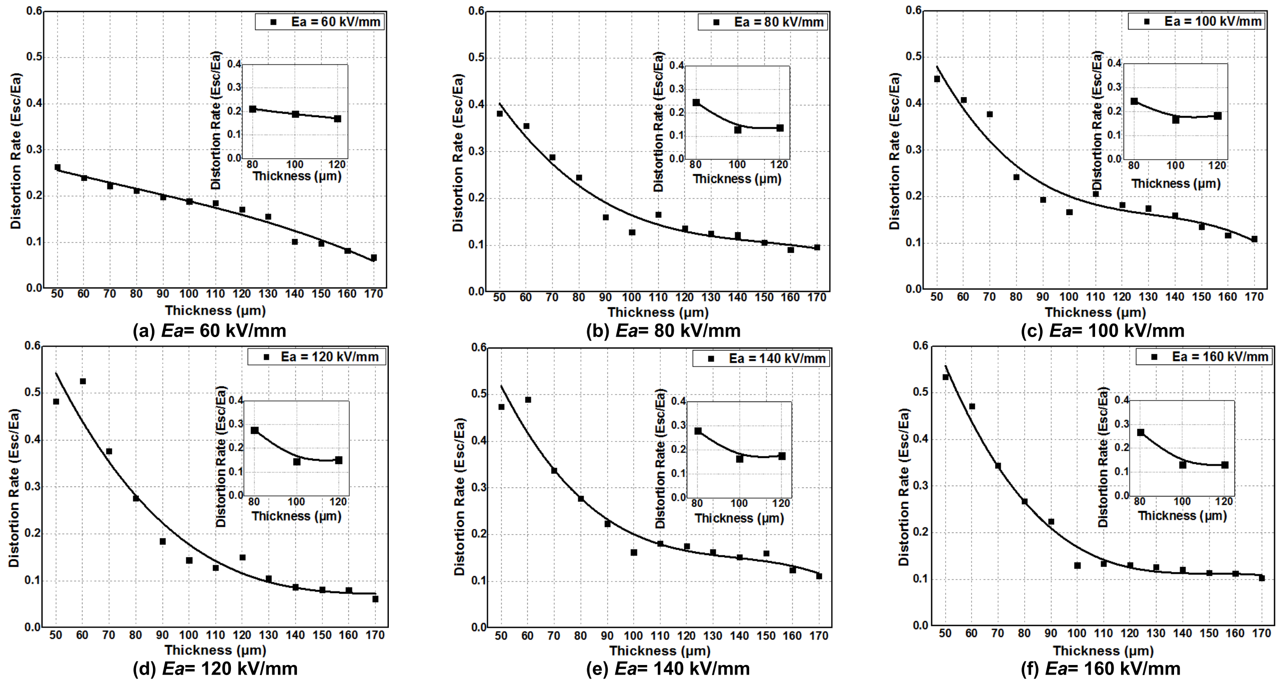

FIGURE 16. **Variation trend of electric field strength distortion rate for different thicknesses under various applied electric field strength.**

behavior and short-time breakdown tests, samples with thicknesses of 50–170 μm were tested in the PEA system.

Unlike the test with the linearly increasing DC voltage used in section III, the constant DC voltage was carried out of the PEA test in this section. The constant E_a were 60, 80, 100, 120, 140, and 160 kV/mm. According to the short-time breakdown test standard, GB/T 1408.1, the duration of DC voltage application should not exceed 20 s. In order to further study the space charge accumulation law when the breakdown occurs, the PEA test time should be selected as the value close to the short-time breakdown test time. The space charge behavior, E_{sc} and E_{real} of the samples were measured after applying the electric field for 20 s.

The PEA test results with the linearly increasing DC voltage shows that the accumulation of space charge is not stable within 0–20s test time as shown in the section III. However, this can not deny the objective phenomenon of space charge accumulation in dielectric. Furthermore, the previous analysis indicates that the regulation of trap characteristics and carrier migration characteristics on the space charge accumulation behavior of the test sample can be clearly analyzed by the space charge test results within 20 s in the third section. The trap characteristics and carrier migration characteristics of dielectric are closely related to the breakdown characteristics. Therefore, for the space charge measurement, the test time of 20 s may cause the charges distribution instability; but for the analysis of dielectric breakdown process, the test results within 20 s contain enough important information that affects the dielectric breakdown characteristics. The effect of space charge behavior on the breakdown characteristics can be obtained by analyzing the variation trend of charge density distribution or electric field distortion within the 20 s after applying test voltage. In fact, there are some of research results to analyze the variation trend of space charge characteristics and obtain the influence rule of some parameters on breakdown characteristics of dielectric. In [21], the phenomenon of packet-like space charge in low-density polyethylene (LDPE) sample before breakdown was studied. The measure time of space charge was less than 2 minutes which did not reach the injection stabilization time. However, this did not prevent the author from clearly measuring and analyzing the packet-like space charge phenomenon. In [36], the effect of pre-stressing on the breakdown characteristics by analyzing the space charge distribution curves of LDPE samples during the breakdown process was studied. The PEA test only lasted for 1 ms.

Fig. 16 shows the variation in the rate of field strength distortion in samples with different thicknesses under various applied field strengths and the results of 80, 100 and 120 μm samples were shown in the second layer of each figure. The variation trend of the field strength distortion rate in the sample is the same, and it decreases with an increase in thickness. However, several differences are observed in the results under various applied field strengths. The distortion rate of samples with $d < 100$ μm is more than 20% (up to 50%), which is much larger than that of samples with $d > 100$ μm, especially when the applied field strength is higher than 100 kV/mm.

The results of 80, 100 and 120 μm samples show that the electric field distortion rate decreases with an increase in thickness which is consistent with the general variation trend. However, in most cases (except for $E_a = 60$ kV/mm), the distortion rate of 100 μm sample is the least of the

three values. This result is related to the regulation of the trap characteristics on the space charge behavior, which has been analyzed previously. Fig. 16 shows that a thin sample has a high field strength distortion rate under high field strength. This occurrence can be explained from the perspective of trap characteristics of samples. The formation of chemical defects is affected to some extent by the size of materials. XLPE with a small thickness or size contains few chemical defects (impurities, cross-linking byproducts, etc.). This condition results in the deep trap density is low for samples with small thickness. The low trap density leads to a large charge accumulation depth, and more charges are injected into the sample bulk, even if the sample itself is very thin. This results in a high field strength distortion rate of the thin sample. For the thick samples, the deep trap density is relatively high, resulting in a small charge accumulation depth, and more charges can not be injected into the sample bulk, even if it is relatively thick. This results in a small field strength distortion rate of the thick sample.

This phenomenon indicates that the analysis of the influence of space charge accumulation on DC breakdown characteristics is reasonable. For thin samples, the high field strength distortion caused by space charge accumulation results in low breakdown field strength. Therefore, in the thickness interval of $d < 100\ \mu$m, the breakdown strength increases with an increase in thickness. In this case, space charge accumulation has an obvious effect on DC breakdown characteristics.

C. ANALYSIS OF DISTORTION FIELD STRENGTH IN THE SAMPLE USING BREAKDOWN STRENGTH

As stated earlier, the sample thickness has an obvious effect on the actual field strength of XLPE samples under an applied field strength. By analyzing the variation trend of the distortion rate, it can be seen that the distortion effect in samples with thicknesses less than 100 μm is more significant than that in samples with thicknesses greater than 100 μm under the same applied field strength. This phenomenon is related to the trend of the breakdown strength observed for different sample thicknesses in AC and DC short-time breakdown tests. Therefore, after breakdown occurs, it is necessary to quantitatively analyze the effect of space charge accumulation on both electric field distortion and breakdown characteristics. In addition, it is necessary to obtain the E_{sc} values using the PEA system until the applied field strength approaches the breakdown strength of the sample. However, this test condition obviously has many contradictions with the normal test conditions employed in the PEA test system. First, the output voltage of the DC source is very high. Taking the DC breakdown strength of the 100 μm sample as an example, shown in Fig. 14(b), the minimum breakdown strength is 302.84 kV/mm, and the corresponding breakdown voltage is 30.3 kV. This shows that the high-voltage DC module of the PEA test system needs to meet the basic requirement of a very high output voltage. Second, a high voltage significantly increases the probability of pre-discharge in the electrode module when the applied field strength is increased by increasing the test voltage. The occurrence of pre-discharge will considerably reduce the accuracy of space charge detection, and repeatability of the test data is difficult to guarantee. Third, it is difficult to guarantee the safety performance of the relevant components in PEA test system under high voltage conditions for a long time. Therefore, it is necessary to gradually increase the applied field strength so that the distortion field strength values obtained near the breakdown values can be used for quantitatively study. The distortion field strength of samples with thickness of 70, 80, 90, 100, 140, and 170 μm was measured after 20 s at applied field strengths of 60, 80, 100, 120, 140, and 160 kV/mm, respectively. The relationship between the distortion field strength and applied electric field strength formed via space charge accumulation can be obtained by solving the conduction current equation shown in (10) in the space charge limited current (SCLC) region [37], [38].

$$j_{SCLC} = \mu_{ext}\rho_{free}(x)\,E_{sc}(x) \tag{10}$$

By introducing the relationship between the free charge density and electric field into (10), it can be written as follows:

$$j_{SCLC} = 4\varepsilon_0\varepsilon_r\upsilon_{ATE}E_{sc}(x)\left(\frac{\alpha_d\varepsilon_0\varepsilon_r}{eN_{t0}}\frac{\partial E_{sc}(x)}{\partial x}\right)^{1/\alpha_d} \tag{11}$$

where j_{SCLC} is the space charge limited current, μ_{ext} is the carrier mobility in extended states, $\rho_{free}(x)$ is the density of free charge, $E_{sc}(x)$ is the internal field strength of the sample formed by space charge accumulation, υ_{ATE} is the carrier-escape frequency in traps, N_{t0} is the exponential pre-term in trap density expressions at energy levels, α_d is the coefficient for characterizing the disorder degree of the medium in relation to ambient temperature. The boundary condition of j_{SCLC} is $E_{sc}(x) = 0$. Based on this boundary condition, the analytical expression for $E_{sc}(x)$ can be obtained by using (11):

$$E_{sc}(x) = \left[(\alpha_d+1)\left(\frac{j_{SCLC}}{4\varepsilon_0\varepsilon_r\upsilon_{ATE}}\right)\frac{q_eN_{t0}}{\alpha_d\varepsilon_0\varepsilon_r}(x+x_0)\right]^{1/(\alpha_d+1)} \tag{12}$$

Equation (12) with undetermined coefficients is written as follows:

$$E_{sc}(x) = [A_F(x+x_0)]^{1/(\alpha_d+1)} \tag{13}$$

The expression for undetermined coefficients A_F can be obtained by integrating (13):

$$A_F^{1/(\alpha_d+1)} = \frac{\alpha_d+2}{\alpha_d+1}\frac{E_ad}{(d+x_0)^{\alpha_d+2/\alpha_d+1}-x_0^{\alpha_d+2/\alpha_d+1}} \tag{14}$$

By introducing (14) into (13), we obtained

$$E_{sc}(x) = \frac{\alpha_d+2}{\alpha_d+1}\frac{E_ad}{(d+x_0)^{\alpha_d+2/\alpha_d+1}-x_0^{\alpha_d+2/\alpha_d+1}} \times (x+x_0)^{1/(\alpha_d+1)} \tag{15}$$

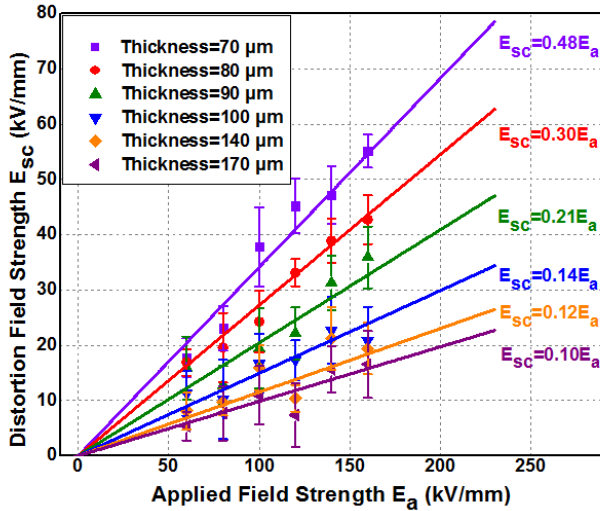

FIGURE 17. Relationship between distortion and applied field strength with different sample thicknesses.

Equation (15) is the analytical expression of the relationship between the distortion field strength (E_{sc}) inside the dielectric and applied field strength (E_a). It can be assumed that E_{sc} is affected by the thickness of the sample and the disorder degree of the dielectric. However, at the same external temperature, the E_{sc} shows a linear relationship with the E_a at a definite position inside the dielectric with a certain thickness. Fig. 17 shows the corresponding relationship between the internal distortion field strength and applied field strength of the samples with different thicknesses.

It can be clearly seen from Fig. 17 that with the increase in sample thickness, the slope of the expression representing the quantitative relationship between E_{sc} and E_a tends to decrease. The decreasing trend of the slope indicates that the effect of the applied field strength on the distortion field strength decreases with an increase in sample thickness. This conforms to the qualitative analysis rule of the field strength distortion rate, that is, the electric field strength distortion caused by the space charge accumulation in the thin sample under high field strength is higher than that of thick sample.

D. QUANTITATIVE ANALYSIS OF DISTORTION FIELD STRENGTH USING EXTRAPOLATION METHOD

The distortion field strength due to space charge accumulation was obtained using the extrapolation method considering the sample breakdown strength. When breakdown occurs, the applied field strength (E_a) of the XLPE is equal to the breakdown strength obtained in the short-time breakdown test. When E_{sc} is obtained, the actual field strength (E_{real}) of samples with different thicknesses can be obtained using (9).

The calculated results of E_a, E_{sc}, and E_{real} are listed in Table 3. Based on the data presented in Table 3, Fig. 18 shows the variation trend of the applied, distortion, and actual field strengths for various sample thicknesses when breakdown occurs. From table 3, E_{sc} is higher than 50 kV/mm and increases with decrease in thickness in the range of $d < 100$ μm. Fig. 18 shows a high distortion field strength in the thin sample under breakdown field strength.

TABLE 3. Calculated results of E_a, E_{sc}, and E_{real}.

Thickness (μm)	E_a (kV/mm)	E_{sc} (kV/mm)	E_{real} (kV/mm)	Standard deviation
70	273.18	131.61	404.79	77.47
80	311.53	94.11	405.64	73.29
90	335.78	70.51	406.29	56.07
100	347.96	52.19	400.15	46.35
110	335.92	50.39	386.31	53.69
120	335.69	50.35	386.04	51.89
130	333.76	43.39	377.15	56.71
140	323.64	38.84	362.48	61.75
150	317.85	38.14	355.99	39.25
160	309.75	34.07	343.82	27.05
170	305.76	30.58	336.34	43.31

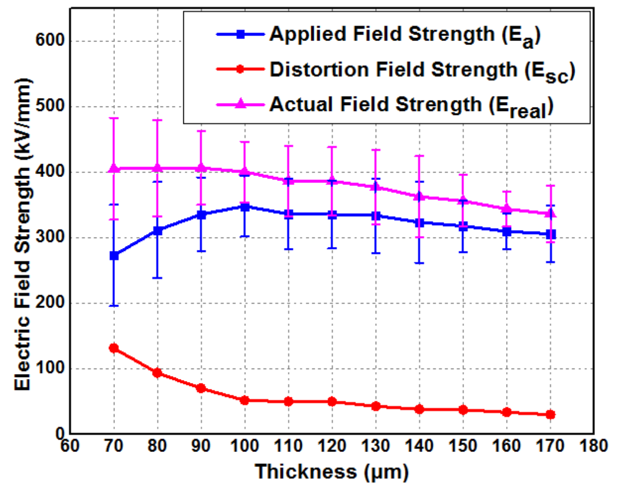

FIGURE 18. Variation trend of Actual (E_{real}), Applied (E_a) and Distortion (E_{sc}) field strength with various thickness when breakdown occurs.

The DC breakdown strength ($E_a = E_{b-dc}$) of XLPE with several thicknesses is affected by the distortion field strength (E_{sc}) when breakdown occurs. The main reason is the high distortion of electric field in the thin sample under high applied electric field. The high distortion field strength results in low breakdown strength. As shown in Fig. 14(b), in the thickness interval of $d < 100$ μm, E_{b-dc} shows a trend of increasing with the increase of thickness. Meanwhile, The trend of E_{sc} decreases with the increasing thickness which is consistent with the result in Fig. 16 when E_a is higher than 100 kV/mm. The decreasing trend represents the weakening of the effect of space charge accumulation on the breakdown characteristics. In the thickness interval of $d > 100$ μm, the variation trend of E_{b-dc} with thickness is in accordance with volume effect.

It can be assumed that if only volume effect affects the breakdown characteristics, the variation trend of breakdown strength with thickness should be consistent with the result of E_{real} in Fig. 18. However, this assumption is not true, because the accumulation of space charge will cause electric field distortion under DC condition. Various thicknesses XLPE samples have different bulk charge accumulation and carrier

migration behaviors, which lead to a decreasing tendency of distortion field strength with an increase in thickness. The effect of space charge behavior in thin samples and volume effect in thick samples are the main reasons for the results of the relationship between E_{b-dc} and sample thickness in Fig.14(b).

V. CONCLUSION

In this paper, the impact of space charge accumulation on the breakdown characteristics of XLPE was analyzed. The space charge behavior in breakdown phenomena was quantitatively analyzed using linear extrapolation, and the distortion field strength was obtained.

Experimental results confirms that AC breakdown strength of XLPE decreases with an increase in thickness due to volume effect, which may influence breakdown process, whereas the DC breakdown strength initially increases and subsequently decreases with an increasing thickness. This phenomenon was related to the distortion in field strength formed by the accumulation of bulk space charges. The space charge behavior, such as injection, migration and accumulation, are the significant factors for the electric field distortion, which are regulated by the trap characteristics of dielectric. The difference in trap characteristics makes the electric field distortion in various thicknesses dielectrics different even under the same applied electric field. This is one of the reasons responsible for the difference of breakdown characteristics with various thicknesses samples, and the other is volume effect.

For XLPE thicknesses less than 100 μm, less chemical defects lead to low density of deep traps, and higher charge accumulation depth due to low injection barrier. More charges accumulate inside the bulk of XLPE. This results in higher distortion rate of field strength, which is 20% larger than applied field strength and finally space charge behavior dominates the breakdown process. However, with an increase in thickness, the density and depth of deep traps increase, which leads to decrease in charge accumulation depth and increases in injection barrier. The charge accumulated inside the dielectric bulk decreases gradually (the minimum amount may appears in the sample with $d = 100$ μm), which also leads to the decrease of electric field distortion. The breakdown strength of XLPE increase with an increase in sample thickness. For XLPE thicknesses greater than 100 μm, the distortion rate of field strength is less than 20% and hence volume effect dominates the breakdown process. The breakdown strength of XLPE decreases with an increase in sample thickness.

Moreover, the effect of space charge accumulation on the long-term voltage-withstanding characteristics of XLPE is not clear, and further studies in this regard will be carried out in future.

REFERENCES

[1] C. W. Reed, "An assessment of material selection for high voltage DC extruded polymer cables," *IEEE Elect. Insul. Mag.*, vol. 33, no. 4, pp. 22–26, Jul. 2017.

[2] X. Liu, Q. Yu, M. Liu, Y. Li, L. Zhong, M. Fu, and S. Hou, "DC electrical breakdown dependence on the radial position of specimens within HVDc XLPE cable insulation," *IEEE Trans. Dielectr. Electr. Insul.*, vol. 24, no. 3, pp. 1476–1484, Jun. 2017.

[3] Y. Liu and X. Cao, "Electrical tree growth characteristics in XLPE cable insulation under DC voltage conditions," *IEEE Trans. Dielectr. Electr. Insul.*, vol. 22, no. 6, pp. 3676–3684, Dec. 2015.

[4] G. Chen, M. Hao, Z. Xu, A. Vaughan, J. Cao, and H. Wang, "Review of high voltage direct current cables," *CSEE J. Power Energy Syst.*, vol. 1, no. 2, pp. 9–21, Jul. 2015.

[5] D. He, X. Wang, H. Liu, Q. Li, and G. Teyssedre, "Space charge behavior in XLPE cable insulation under AC stress and its relation to thermo-electrical aging," *IEEE Trans. Dielectr. Electr. Insul.*, vol. 25, no. 2, pp. 541–550, Apr. 2018.

[6] J. Li, Y. Gao, Y. Q. Yuan, S. H. Huang, and B. X. Du, "Space charge accumulation inPolypropylene/Elastomer blends with different elastomer types," in *Proc. IEEE 2nd Int. Conf. Dielectr. (ICD)*, Jul. 2018, pp. 1–4.

[7] M. Sepulveda-Garcia, J. Martinez-Tarifa, and J. Sanz-Feito, "Electrical ageing markers for polyethylene insulation based on space charge accumulation and apparent mobility," *IEEE Trans. Dielectr. Electr. Insul.*, vol. 20, no. 6, pp. 2222–2229, Dec. 2013.

[8] S. Mitsumoto, K. Tanaka, Y. Muramoto, M. Nagao, N. Hozumi, and M. Fukuma, "Space charge distribution measured with short period interval up to electrical breakdown in polyethylene," in *Proc. Annu. Rep. Conf. Electr. Insul. Dielectr. Phenomena (CEIDP)*, vol. 2, 1999, pp. 634–637.

[9] Y. Li and T. Takada, "Progress in space charge measurement of solid insulating materials in Japan," *IEEE Elect. Insul. Mag.*, vol. 10, no. 5, pp. 16–28, Sep. 1994.

[10] S. Delpino, D. Fabiani, G. C. Montanari, L. A. Dissado, C. Laurent, and G. Teyssedre, "Fast charge packet dynamics in XLPE insulated cable models," in *Proc. Annu. Rep.-Conf. Electr. Insul. Dielectric Phenomena (CEIDP)*, 2007, pp. 421–424.

[11] Z. Lv, S. M. Rowland, and K. Wu, "Simulation of fast space charge packets transport in polymers," in *Proc. IEEE Conf. Electr. Insul. Dielectr. Phenomenon (CEIDP)*, Oct. 2017, pp. 98–101.

[12] T. Christen, "The effect of injection properties of contacts on the dynamics of unipolar space-charge limited currents," *IEEE Trans. Dielectr. Electr. Insul.*, vol. 23, no. 6, pp. 3712–3724, Dec. 2016.

[13] Y. Wang, J. Wu, and Y. Yin, "A space-charge and relaxation-current based method for estimating electron and hole trap energy distribution," *IEEE Trans. Dielectr. Electr. Insul.*, vol. 24, no. 6, pp. 3839–3848, Dec. 2017.

[14] *Standard Test Method for Dielectric Breakdown Voltage and Dielectric Strength of Solid Electrical Insulating Materials at Commercial Power Frequencies*, Standard ASTM-D149-2009, 2009.

[15] *Standard Electrical strength of insulating materials-Test methods—Part 1: Test at Power Frequencies*, Standard GB/T 1408.1-2006, Sep. 2006.

[16] T. Mizutani, Y. Suzuoki, M. Hanai, and M. Ieda, "Determination of trapping parameters from TSC in polyethylene," *Jpn. J. Appl. Phys.*, vol. 21, no. 11, pp. 1639–1641, Nov. 1982.

[17] F. Tian, W. Bu, L. Shi, C. Yang, Y. Wang, and Q. Lei, "Theory of modified thermally stimulated current and direct determination of trap level distribution," *J. Electrostatics*, vol. 69, no. 1, pp. 7–10, Feb. 2011.

[18] J. Su, B. Du, T. Han, Z. Li, M. Xiao, and J. Li, "Multistep and multiscale electron trapping for high-efficiency modulation of electrical degradation in polymer dielectrics," *J. Phys. Chem. C*, vol. 123, no. 12, pp. 7045–7053, Mar. 2019.

[19] P. Molinie, "A review of mechanisms and models accounting for surface potential decay," *IEEE Trans. Plasma Sci.*, vol. 40, no. 2, pp. 167–176, Feb. 2012.

[20] M. Fukuma, K. Fukunaga, and T. Maeno, "Space charge dynamics in LDPE films immediately before breakdown," *IEEE Trans. Dielectr. Electr. Insul.*, vol. 8, no. 2, pp. 304–306, Apr. 2001.

[21] L. Zhang, Y. Zhou, C. Teng, Y. Zhang, M. Chen, and Z. Cheng, "Transient dynamics of packet-like space charge in low-density polyethylene at high temperatures," *J. Electrostatics*, vol. 88, pp. 100–105, Aug. 2017.

[22] Y. X. Zhou, N. H. Wang, and Y. S. Wang, "Review of research on space charge in solid dielectrics," *Trans. China Electrotech. Society.*, vol. 23, no. 9, pp. 16–25, Sep. 2008.

[23] T. Takada, "Acoustic and optical methods for measuring electric charge distributions in dielectrics," in *Proc. Annu. Rep. Conf. Electr. Insul. Dielectr. Phenom. (CEIDP)*, 1999, pp. 1–14.

[24] F. Tian and C. Hou, "A trap regulated space charge suppression model for LDPE based nanocomposites by simulation and experiment," *IEEE Trans. Dielectr. Electr. Insul.*, vol. 25, no. 6, pp. 2169–2177, Dec. 2018.

[25] S. Li, D. Min, W. Wang, and G. Chen, "Modelling of dielectric breakdown through charge dynamics for polymer nanocomposites," *IEEE Trans. Dielectr. Electr. Insul.*, vol. 23, no. 6, pp. 3476–3485, Dec. 2016.

[26] J. G. Simmons, "Conduction in thin dielectric films," *J. Phys. D, Appl. Phys.*, vol. 4, no. 5, pp. 613–657, May 1971.

[27] *Standard Pulsed Electro-Acoustic Test Method for Space Charge Measurement in Solid Insulating Materials*, Standard JB/T 12927-2016, 2016.

[28] K. Wu, Y. Wang, Y. Cheng, and L. A. Dissado, "Connection between disorder in morphology and stochastic nature of electrical breakdown in insulating polymers," in *Proc. 10th IEEE Int. Conf. Solid Dielectrics (ICSD)*, Jul. 2010, pp. 1–4.

[29] S. M. Hasheminezhad, E. Ildstad, and A. Nysveen, "Breakdown strength of solid|solid interface," in *Proc. 10th IEEE Int. Conf. Solid Dielectr. (ICSD)*, Jul. 2010, pp. 1–7.

[30] B. Helgee and P. Bjellheim, "Electric breakdown strength of aromatic polymers: Dependence on film thickness and chemical structure," *IEEE Trans. Electr. Insul.*, vol. 26, no. 6, pp. 1147–1152, Dec. 1991.

[31] U. Riechert, M. Eberhardt, and J. Kindersberger, "Breakdown behavior of polyethylene at DC voltage stress," in *Proc. IEEE Int. Conf. Solid Dielectr. (ICSD)*, Jun. 1998, pp. 510–513.

[32] Y. Murakami and G. Chen, "Influence of film thickness on space charge formation under DC ramp voltage," in *Proc. IEEE Int. Conf. Solid Dielectr. (ICSD)*, Jun. 2013, pp. 448–451.

[33] L. Z. Wang, "Effect of voltage waveform and thickness of sample on breakdown voltage strength," *Telecommun. Eng.*, no. 4, pp. 98–101, 1981.

[34] R. Khazaka, M. Bechara, S. Diaham, and M.-L. Locatelli, "Parameters affecting the DC breakdown strength of parylene F thin films," in *Proc. Annu. Rep. Conf. Electr. Insul. Dielectr. Phenomena (CEIDP)*, Oct. 2011, pp. 740–743.

[35] S. Konzelmann and D. Peier, "Electric strength and dieletric properties of μm-polymer-films," in *Proc. 10th IEEE Int. Conf. Solid Dielectr. (ICSD)*, Jul. 2010, pp. 1–4.

[36] M. Fukuma, T. Maeno, K. Fukunaga, and M. Nagao, "High repetition rate PEA system for *in-situ* space charge measurement during breakdown tests," *IEEE Trans. Dielectr. Electr. Insul.*, vol. 11, no. 1, pp. 155–159, Feb. 2004.

[37] L. A. Dissado and J. C. Fothergill, *Electrical Degradation and Breakdown in Polymers*. Stevenage, U.K.: Peregrinus, 1992, pp. 452–476.

[38] D. M. Min, "Investigation into charge trapping transport properties and mechanisms in polymeric insulating materials," Ph.D. dissertation, Dept. Elect. Eng., Xi'an Jiaotong Univ., Xi'an, China, 2013.

ZHIPENG MA was born in China, in 1988. He is currently pursuing the Ph.D. degree with the College of Electrical Engineering, Chongqing University, China. His major research interests are in influence of space charge on insulation characteristics of cable breakdown and dielectric behavior of insulation material.

LIJUN YANG (Member, IEEE) was born in China, in 1980. She received the M.S. and Ph.D. degrees in electrical engineering from Chongqing University, China. She is currently a Professor with the Electrical Engineering College, Chongqing University. Her research interests are in the field of on-line monitoring of insulation condition and fault diagnosis for high voltage apparatus, as well as aging mechanism and diagnosis for power transformer.

MUHAMMAD SHOAIB BHUTTA was born in Pakistan, in April 1988. He received the M.Sc. degree in electrical engineering from Chongqing University, Chongqing, China, in 2014, where he is currently pursuing the Ph.D. degree. His research interests are in high voltage and its insulation includes high voltage direct current insulation, nano dielectric, and breakdown testing and dielectric failure mechanisms.

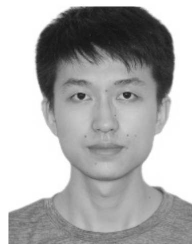

HAORAN BIAN was born in China, in 1994. He is currently pursuing the Ph.D. degree with the College of Electrical Engineering, Chongqing University, China. His major research interests include the field of aging mechanism and space charge effect for power cable.

MUHAMMAD ZEESHAN KHAN received the B.S. degree in electrical engineering from CIIT ATD, Pakistan, and the M.S. degree in electrical engineering from Chongqing University, Chongqing, China, in 2015, where he is currently pursuing the Ph.D. degree. His major research interest is in dielectric electrical insulation.